Bilayer structure and physical dynamics of the cytochrome b_5 dimyristoylphosphatidylcholine interaction

David W. Chester,*‡ V. Skita,* H. S. Young,‡ T. Mavromoustakos,§ and P. Strittmatter‡
*Biomolecular Structure Analysis Center, and ‡Department of Biochemistry, University of Connecticut Health Center, Farmington, Connecticut 06030; and §Institute of Material Science, University of Connecticut, Storrs, Connecticut 06268

ABSTRACT Cytochrome b_5 is a microsomal membrane protein which provides reducing potential to Δ^5-, Δ^6- and Δ^9-fatty acid desaturases through its interaction with cytochrome b_5 reductase. Low angle x-ray diffraction has been used to determine the structure of an asymmetrically reconstituted cytochrome b_5:DMPC model membrane system. Differential scanning calorimetry and fluorescence anisotropy studies were performed to examine the bilayer physical dynamics of this reconstituted system. These latter studies allow us to constrain structural models to those which are consistent with physical dynamics data. Additionally, because the nonpolar peptide secondary structure remains unclear, we tested the sensitivity of our model to different nonpolar peptide domain configurations. In this modeling approach, the nonpolar peptide moiety was arranged in the membrane to meet such chemically determined criteria as protease susceptibility of carboxyl- and amino-termini, tyrosine availability for pH titration and tryptophan 109 location, et cetera. In these studies, we have obtained a reconstituted cytochrome b_5:DMPC bilayer structure at ~6.3 Å resolution and conclude that the nonpolar peptide does not penetrate beyond the bilayer midplane. Structural correlations with calorimetry, fluorescence anisotropy and acyl chain packing data suggest that asymmetric cytochrome b_5 incorporation into the bilayer increases acyl chain order. Additionally, we suggest that the heme peptide:bilayer interaction facilitates a discreet heme peptide orientation which would be dependent upon phospholipid headgroup composition.

INTRODUCTION

Cytochrome b_5, located on the cytoplasmic face of the endoplasmic reticulum membrane, functions as part of the fatty acid desaturase complex responsible for the production of both mono- and polyunsaturated fatty acids. As such, the desaturase complex is responsible for modulation of membrane physical dynamics as well as production of fatty acid pools for second messenger synthesis (cyclooxygenase pathway). Within the complex, cytochrome b_5 serves to shuttle, via a diffusion dependent process, reducing potential from the cytochrome b_5 reductase to the Δ^5-, Δ^6- and Δ^9-desaturases (Lee et al., 1977, Okayasu et al., 1977). Desaturase nonheme iron reduction by cytochrome b_5 electron transfer initiates the desaturation process by a mechanism which remains to be elucidated (Strittmatter et al., 1974, Jeffcoat and James, 1984). Cytochrome b_5 has also been implicated as a participant in fatty acyl chain elongation (Keyes et al., 1979), fatty acid retroconversion and cholesterol biosynthesis (Reddy et al., 1977). The structural organization of the components of the desaturase complex, as well as the physical dynamics of the protein-lipid interaction, are therefore essential to an understanding of the mechanisms involved in lipid desaturation and subsequent maintenance of bilayer integrity, fluid dynamics and function.

Address correspondence to Dr. Chester.

Cytochrome b_5 is a 16,700 D molecular weight protein containing two functional domains: catalytic heme peptide and nonpolar-membrane binding segment (NPP; Spatz and Strittmatter, 1971). The (oxidized) heme peptide crystal structure has been solved to ~2 Å resolution by Mathews et al. (1979, Fig. 5). NMR studies on the heme peptide in solution demonstrate that the observed crystal structure is conserved in free solution and independent of heme iron oxidation state (Veitch et al., 1988). While no direct NPP structural data have been obtained, primary sequence (Ozols, 1989), CD (Dailey and Strittmatter, 1978) and FTIR spectroscopy (Holloway and Mantsch, 1989) have been used to suggest structural motifs. CD spectral data (Dailey and Strittmatter, 1978) obtained from membrane bound NPP suggest a secondary structure containing ~50% α-helix, 25% β-sheet and 25% random coil (Dailey and Strittmatter, 1978). In addition, Fleming et al. (1978) suggested that the β-sheet structure is most likely organized into a 3_{10}-helix conformation. Recent FTIR solution studies on both holo and TPCK-Trypsin cleaved cytochrome b_5 peptides suggest a NPP structure consisting of 43% α-helix, 33% β-sheet, 12% β-turns and 12% random coil (Holloway and Mantsch, 1989). Additional FTIR studies on membrane bound NPP suggest a structure containing ~56% α-helical content (Holloway and Bucheit, 1990).

0006-3495/92/05/1224/20 $2.00

In evaluating the NPP structural organization within the bilayer, Dailey and Strittmatter (1981) proposed a *cis* model where tightly bound cytochrome b_5 carboxyl- and amino-termini reside on the same side of the membrane. Alternatively, Takagaki et al. (1983*a*, *b*) postulated a *trans* configuration where amino- and carboxyl-termini reside on opposing sides of the membrane. The *cis* orientation is supported by several studies evaluating carboxyl-terminal residue accessibility (Ozols, 1989, Dailey and Strittmatter, 1981, Arinc et al., 1987). Brominated-lipid tryptophan fluorescence quenching experiments of Everett et al. (1986) are also consistent with a *cis* orientation. To date, x-ray (Rzepecki et al., 1986) and neutron (Gogol et al., 1983, Gogol and Engelman, 1984) diffraction studies on membrane bound cytochrome b_5 have been unable to discriminate between these two NPP structural configurations. Low resolution (15 Å) x-ray studies reveal an asymmetric bilayer structure which is consistent with NPP penetration to the bilayer center (Rzepecki et al., 1986). This model is qualitatively consistent with calorimetry and resonance energy transfer studies suggesting that only one monolayer is perturbed by asymmetric cytochrome b_5 incorporation (Friere et al., 1983). In contrast, modeling of low resolution ($\sim$29 Å) neutron scattering data suggest that the NPP penetrates through the bilayer (Gogol et al., 1983, Gogol and Engelman, 1984).

The present study attempts to examine the DMPC bilayer/cytochrome b_5 structure at significantly higher resolution than previously attained. We have obtained an phased lamellar x-ray diffraction data to $\sim$6.3 Å resolution to obtain a relative electron density profile structure of the asymmetrically reconstituted cytochrome b_5:DMPC membrane. Differential scanning calorimetry, fluorescence anisotropy and fatty acyl chain packing studies were performed to evaluate the bilayer physical dynamics of this asymmetric system and constrain our model interpretations. Our structure data demonstrate that, in this tightly bound asymmetrically reconstituted cytochrome b_5 system, the NPP does not penetrate significantly beyond the bilayer midplane. Physical dynamics data demonstrate an increase in acyl chain order both above and below the membrane thermal phase transition as a consequence of asymmetric cytochrome b_5 insertion.

MATERIALS AND METHODS

Membrane preparation

Dimyristoylphosphatidylcholine (DMPC, Avanti Polar Lipids, Birmingham, AL) large unilamellar vesicles (LUV) were prepared by either of the two detergent dilution methods (small unilamellar vesicle fusion or mixed detergent:lipid micelle formation) described by Enoch and Strittmatter (1979). We did note substantial LUV size dependence on cation concentration and, therefore, used a higher initial salt concentration (150 mM) to facilitate larger vesicle formation. The DMPC lipid suspension (40 μM/ml) was prepared in 0.5 mM Hepes, 150 mM NaCl buffer, pH 8.1 and warmed to 41°C before sonication. In both cases, a 1:6 sodium deoxycholate (DOC, Aldrich Chemical Co., Inc., Madison, WI):DMPC mole ratio was used in LUV formation. Detergent was removed by slow passage down a Sephadex G-50 column (Pharmacia AB Biotechnology, Uppsala, Sweden) with the temperature set to 42°C to facilitate detergent flip-flop. Vesicle phosphate concentration was determined as described by Chester et al. (1986). Vesicles prepared by this method are typically 800–1,000 Å in diameter as demonstrated by negative staining with 1% uranylacetate (see Fig. 1). The vesicle preparation was then desalted to 20 mM NaCl, 0.5 mM Hepes, pH 8.1 over Sephadex G-25 before reconstitution.

Lipid and cytochrome b_5 purity were demonstrated by thin layer and gel filtration chromatography/absorption spectrum, respectively, before use. Additionally, chromatographic evaluation of DMPC integrity after diffraction yielded a single spot, demonstrating that lipid breakdown was not occuring during data collection. Similarly, cytochrome b_5 redox potential could be recovered from detergent solubilized diffraction samples.

Cytochrome b_5 binding to DMPC LUV

Asymmetric reconstitution was accomplished by addition of Black Angus Steer cytochrome b_5 (in 20 mM Tris:Acetate, pH 8.1) to preformed DMPC vesicles at selected mole ratios to obtain the desired packing density. Vesicle surface saturating cytochrome b_5 concentrations were used for the bulk of these studies unless otherwise stated. Reconstitution was carried out for 8–12 h at 32°C to ensure "tight" cytochrome b_5 binding (Enoch et al., 1979). Bound and free cytochrome b_5 were separated by gel filtration chromatography (Sephacryl S-400 HR, Pharmacia AB Biotechnology) and DMPC:cytochrome b_5 ratios determined by phosphate assay and Soret absorption (millimolar extinction of 117 L $mM^{-1}cm^{-1}$ at 413 nm). Reconstitution asymmetry was verified by assaying cytochrome b_5-reductase:NADH mediated cytochrome b_5 reduction (typically, 5–10 μM cytochrome b_5; 18 μg/ml NADH, 1 μM cytochrome b_5 reductase) at 424 nm in the presence and absence of 3.5 mM deoxycholate. Vesicles were maintained at 4°C before use and under these conditions, cytochrome b_5 asymmetry and vesicle integrity remained stable.

Because the spin dry process (Chester et al., 1986) was used in diffraction sample preparation, DMPC:cytochrome b_5 LUVs were desalted to 5 mM NaCl before sedimentation, thus maintaining physiological salt concentrations in the final partially hydrated multilayer stacks. Reconstituted vesicles used in fluorescence and calorimetry studies (in solution) were maintained at 150 mM NaCl. We must note, that for most of the diffraction studies, vesicle formation and cytochrome b_5 reconstitution were performed under 20 mM NaCl conditions which tended to yield slightly smaller diameter vesicles. Under these reconstitution conditions, however, the lipid:cytochrome b_5 ratios, protein asymmetry, et cetera were conserved. Further, we assumed that formation of extended multilamellar membrane stacks from these vesicles would reduce acyl chain and protein packing constraints anticipated in vesicles with a smaller radius of curvature.

Membrane multilayer preparation

Multilayer membranes were prepared by the spin dry method described by Chester et al. (1986) as adopted from Clark et al. (1980). Partially hydrated multilayers for use in lamellar scatter experiments were mounted on curved glass supports and rehydrated to 90% relative humidity ($ZnSo_4 \cdot 7\ H_2O$) for a period of 12–15 h at room temperature in sealed brass specimen canisters. Subsequent changes

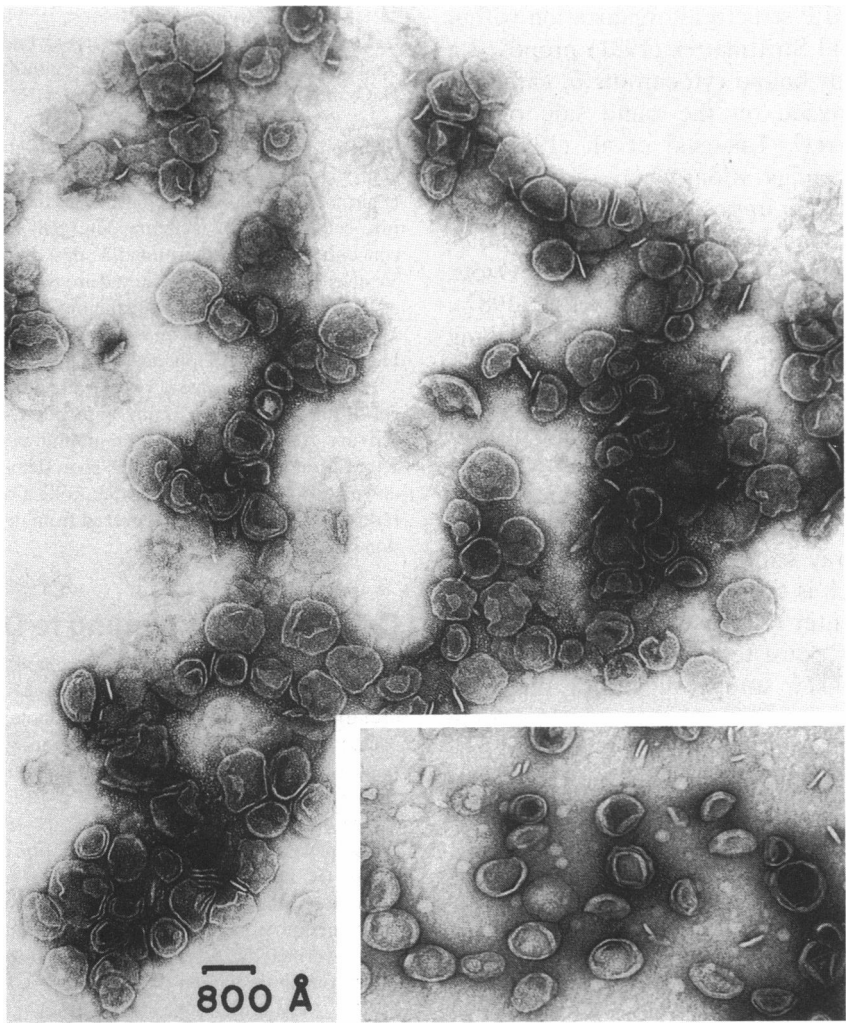

FIGURE 1 Negative stained DMPC large unilamellar vesicles reconstituted asymmetrically with cytochrome b_5 at a protein to lipid ratio of 1:30. (*Inset*) DMPC vesicles before the reconstitution process.

in bilayer hydration were performed for a minimum of 3 h at 25°C to facilitate complete equilibration and sample stabilization.

Membrane multilayers for equatorial scatter studies were removed from the substrates and deposited onto Butvar (Polyvinyl-Butyral Resin, Polysciences, Inc., Warrington, PA) coated (30–60-nm thickness) nickel slotted electron microscopy grids (1.2 × 2.0 mm slot, Polysciences, Inc., Warrington, PA). Control DMPC multilayer samples were prepared by depositing a hanging drop of concentrated vesicles on the Butvar coated grids and, subsequently dehydrating over saturated LiCl (13% relative humidity) for several hours. These samples were rehydrated to 90% in the same manner described for lamellar scatter.

Diffraction

Samples were temperature equilibrated on the beamline for 1 h before data collection. An Elliott GX-18 Rotating Anode x-ray Generator (Marconi Avionics, Ltd., United Kingdom) provided Cu K x-rays which were line focused with a single Franks' mirror (lamellar scatter) or point focused with a double Franks' mirror (equatorial scatter). K_β radiation was filtered with Ni foil leaving K_α x-rays (λ = 1.54 Å). Sample temperature was maintained with a Neslab 4B circulating water bath (Neslab Instruments Inc., Newington, NH) and monitored with a thermistor probe mounted on the sample housing. Background scatter was reduced with He filled beam paths. In all cases, samples were translated into the x-ray beam until the beam intensity was reduced by 20%.

Either a Braun Position Sensitive Detector (PSD; Innovative Technologies, Inc., MA) or DEF-5 x-ray film stack (Eastman Kodak, NY) was used to measure x-ray scatter. High angle lamellar scattering data were collected by moving the detector arm in 2θ. Care was taken to ensure sufficient reflection overlap such that relative intensities could be properly scaled. Sample mosaic spread and, hence, reflection: detector face intersection geometry was evaluated from film data. These considerations were important to obtaining correct intensity functions for integration and analysis. The film data also allowed us to confirm the presence and relative amplitudes of the higher angle reflections (see Fig. 2*a*, and *b*) and identify camera and beam tunnel scattering artifacts.

In equatorial scattering experiments, partially hydrated multilayers

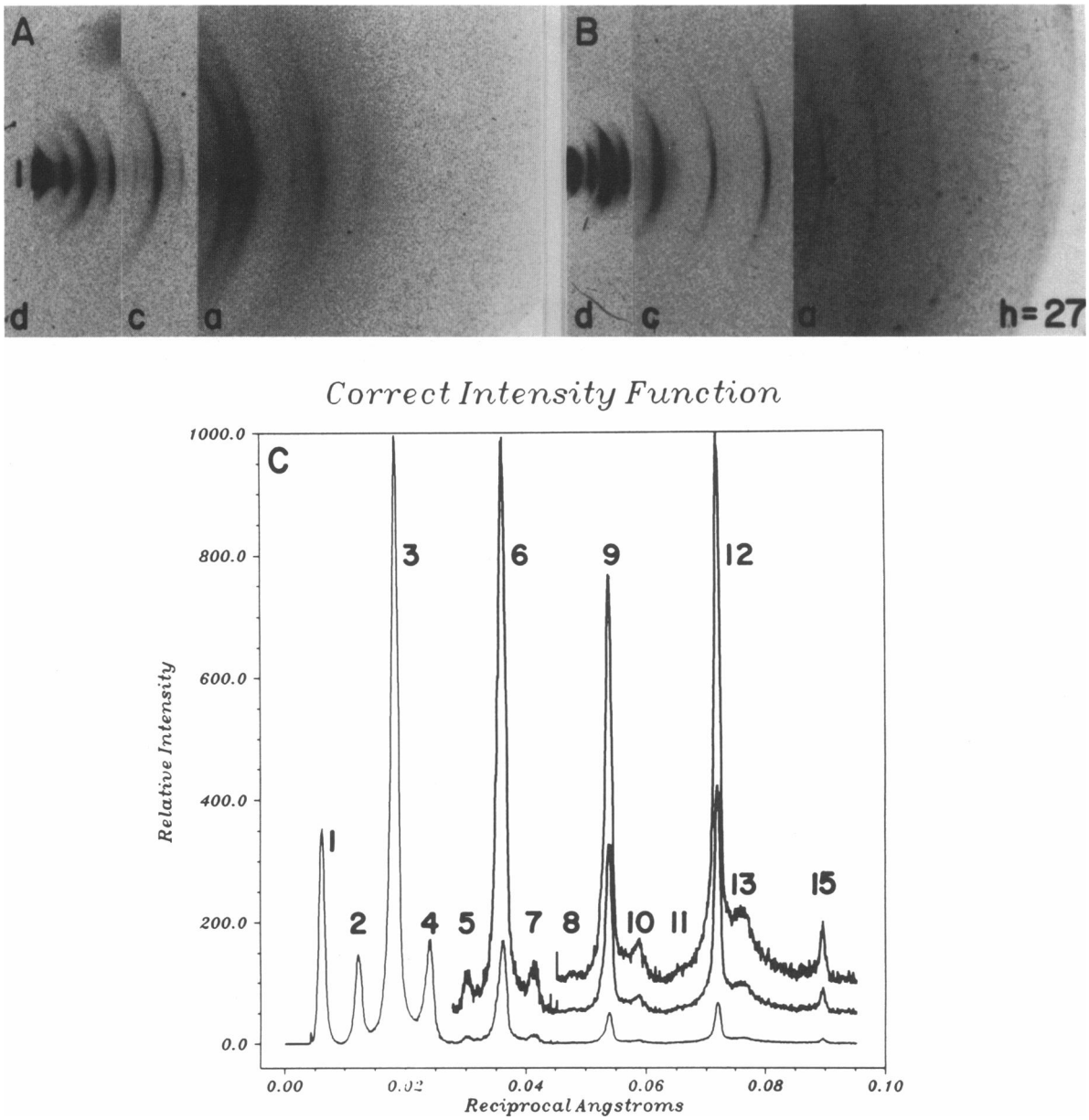

FIGURE 2 Lamellar diffraction patterns from the asymmetrically reconstituted cytochrome b_5:DMPC bilayers. The film patterns shown in Fig. 2 *a* and *b* are represented as segments of films within the film stack. (*a*) typical film pattern from a sample equilibrated to 90% relative humidity and repeat spacing of 176.3 Å. Note the presence of the beam profile in this pattern and the $1/e$ width of each reflection as evidence for the lack of significant sample lattice disorder. (*b*) film pattern from a sample equilibrated to 84% relative humidity and repeat spacing of 170.1 Å. The highest angle reflection observed, $h = 27$ is highlighted. (*c*) correct lamellar intensity function derived from the geometrically corrected detector pattern from the sample used to generate the film pattern in Fig. 2 *b*.

mounted on coated EM grids were oriented perpendicular to a point focused x-ray beam and equatorial scatter collected on DEF-5 film. Sample temperature was continuously monitored during the course of 2 h data collection. Scatter controls (Butvar coated grid only) were run to demonstrate the absence of coherent scatter from the 30–60-nm thick Butvar resin substrate.

Sample stability was assessed by recording a series of 5 min diffraction patterns at constant x-ray flux over an 8 h period. No changes were observed in either reflection amplitudes or positions during this time.

Data analysis and reduction

A data analysis and reduction package, affectionately referred to as the PENN Programs (Developed by R. Fischetti and V. Skita, University of Pennsylvania, 1985, and, subsequently, developed and

modified by V. Skita, University of Connecticut Health Center), was used throughout for 1-dimensional detector data analysis. The PSD was routinely calibrated for linearity and uniformity. The raw intensity data was converted to units of s ($s = 2 \sin \theta/\lambda$), where 2θ is the angle between the incident and scattered beam for a particular reflection. These experimental intensity data, $I_{exp}(s)$, were background corrected with a sum of exponentials. Substantial agreement was obtained between the summed exponential used to correct $I_{exp}(s)$ and the scattering background in the absence of sample. Lorentz corrections and corrections due to mosaic spread were applied to the background corrected $I_{exp}(s)$ as detailed in Results, yielding $I_{cor}(s)$.

Film data were scanned along the fiducial and peak intensities integrated with a $\sim 20 \times 200$ μ focused Zeineh 2-DSUV soft laser densitometer (Biomed Instruments, Inc., Fullerton, CA). Because the recorded arcs were typically on the order of 15-mm wide, the background corrected intensities occurring at h/d (h = Bragg index, d = unit cell repeat spacing) were corrected by a factor of $(2 \sin \theta/\lambda)^2$. As detailed in Results, the corrected film intensity data were compared with integrated $I_{cor}(s)$ as a means of validating the appropriateness of geometric corrections to detector data.

Phasing of the intensity data was accomplished by a combination of several basic approaches and will be discussed in Results.

Differential scanning calorimetry (dsc)

Differential scanning calorimetry studies were performed on a Perkin-Elmer DSC-7 (Perkin-Elmer, Newton, CT). Dsc data were collected on 800–1,000 Å DMPC LUVs in the presence and absence of asymmetrically reconstituted cytochrome b_5. LUVs were prepared as described previously with cytochrome b_5:lipid ratios ranging from 1:29 to 1:78 and concentrated to appropriately 40 mg/ml using Centricon-30 filters (Amicon, Danvers, MA). Because it was our desire to correlate thermotropic behavior with our structure determinations, 50-μl aliquots of concentrated vesicles were placed in aluminum dsc pans and samples maintained either in excess water (buffer) or dehydrated to 90% relative humidity (equilibration over saturated $ZnSO_4 \cdot 7\ H_2O$, 24 h). Sealed dsc samples were stored at 4°C before scanning to maintain constant sample thermal history for each data set. Heating and cooling scans were performed at a rate of 2.5°C/min over the temperature range of 10–45°C. While there was the anticipated hysteresis in heating/cooling scans, there was no observed hysteresis upon rescanning in either direction.

Fluorescence anisotropy

DMPC 800–1,000 Å LUVs were prepared as described above. Before cytochrome b_5 reconstitution, the vesicles were incubated with a 1:1000 mole ratio of either 1,6-diphenyl-hexatriene (DPH) or perylene for 60 min at 35°C. Asymmetric cytochrome b_5 reconstitution proceeded as described above and yielded similar cytochrome b_5:lipid ratios. Fluorescence anisotropy data were collected on an SLM-8000C Fluorescence Spectrophotometer (SLM Instruments, Urbana, IL) equipped with polarizers in the excitation and emissions beam ports. Excitation and emissions wavelengths used for DPH and Perylene were 357/430 nm and 436/474 nm, respectively. The sample housing was continuously N_2 flushed to eliminate both low temperature mediated cuvette fogging and oxygen mediated fluorescence quenching. In addition, the excitation shutter was closed between measurements to minimize the potential for probe photobleaching. Sample temperature (range 12–40°C) was maintained by an Endocal circulating waterbath (Neslab Instruments Inc., Newington, NH) and continuously monitored. Each data set was corrected for vesicle scatter by evaluating the parallel and perpendicular scattering components of unlabelled vesicles under identical PMT voltage/gain conditions.

Molecular modeling

The PDB data base (Brookhaven National Laboratories, Upton, NY) cytochrome b_5 heme peptide (oxidized) and phospholipid crystal structures of Mathews et al. (1979) and Pearson and Pascher (1979), respectively, were used on an Evans and Sutherland PS300 (Evans and Sutherland Computer Corp., Salt Lake City, Utah) operating with the CHEMX software package (Chemical Design, Ltd., Oxford, England) to generate model lipid:protein bilayers. Given the heme peptide α-helical content organization, relative bilayer affinity for α-helices, and the cytochrome c orientation determined by Pachence et al. (1990), the membrane:heme peptide interaction was modeled with the heme plane parallel to the bilayer surface. In our initial approach, the bilayer was modeled with 16 lipids and 1 heme peptide (see Fig. 5 *a*) and the electron density profile, $\rho(z)$, generated using an algorithm developed by Blechner et al. (1991) where $\rho(z) = \int\int \rho(x, y, z)\, dxdy$ with the z-axis normal to the bilayer plane. The strip model in Fig. 5 *b* was constructed from relative amplitudes of different bilayer regions which were adjusted to account for the lipid: cytochrome b_5 ratio and anticipated bilayer asymmetry. In addition, the interlamellar spaces were modelled to include water. The average electron density of the strip model was set to zero and this function transformed to generate the $F(s)$ shown in Fig. 5 *c*.

Subsequent model building, described fully in Discussion, was used to evaluate the sensitivity of our structural model to different NPP configurations (Fig. 10). In these models, the CHEMX amino acid data base was used to build several NPP structures from primary sequence and spectroscopic data presented elsewhere (Ozols, 1989, Dailey and Strittmatter, 1978, Holloway and Mantsch, 1989). These NPP moieties were ligated to the heme peptide and bilayers constructed considering both lipid:protein ratio and biochemical constraints (e.g., tyrosine pH titration, tryptic cleavage, et cetera). This criterion for model success or failure was based on comparison of the model $\rho(z)$ with the experimentally determined $\rho(z)$.

The cytochrome b_5 surface electric charge potential was determined using the default CHEMX amino acid charge parameters.

RESULTS

These studies have, as their focus, the determination of the asymmetrically reconstituted cytochrome b_5:DMPC bilayer structure. Specifically, we are interested in determining whether the NPP of holo-cytochrome b_5 is in the *cis* or *trans* configuration. Strittmatter and Rogers (1975) have previously demonstrated functional cytochrome b_5 reconstitution into DMPC small unilamellar vesicles. There are several distinct advantages to a DMPC membrane reconstitution system: increased order inherent to disaturated lipid system, sample stability, and a well established thermotropic behavior. As such, this system should yield enhanced structural resolution and the ability to examine asymmetric protein incorporation effects on bilayer physical dynamics. In essence, then, we can constrain structural models derived from diffraction

studies to be consistent with physical dynamics measurements.

Vesicle characterization is imperative because we wish to cross correlate structure data obtained from partially hydrated planar membrane multilayers with physical dynamics data from vesicles in solution. Essentially two conditions must be met by the reconstituted DMPC vesicle preparation: stable asymmetric cytochrome b_5 incorporation and minimum vesicle diameter limit. Vesicle diameter in part determines the vesicle's radius of curvature which has a measured effect on calorimetric and fluorescence assessments of bilayer physical dynamics and thus, on our ability to extrapolate these data to fully extended bilayers. Stable unidirectional protein reconstitution is also necessary if we are to determine the peptide mass distribution along the centrosymmetric double membrane normal.

Asymmetric cytochrome b_5 reconstituted DMPC vesicles are shown in Fig. 1 where the inset represents DMPC LUV used in the reconstitution process. These vesicles range in size from 800 to 1,000 Å in diameter and have a cytochrome b_5:lipid ratio of 1:30 ± 2. A thorough evaluation of the vesicle preparation by negative staining failed to detect the presence of significant multilamellar vesicle contamination which would tend to cause the appearance of a second lamellar repeat solely due to DMPC at ~58 Å in subsequent x-ray diffraction experiments. It is clear that neither vesicle size nor integrity were altered by incorporation of surface saturating cytochrome b_5 concentrations. Cytochrome b_5 titration curves (data not shown) demonstrate vesicle surface saturation to occur at a protein:lipid ratio of 1:29, a value consistent with measurements made by Rzepecki et al. (1986) in an eggPC system. Because cytochrome b_5 reconstitution is accomplished by protein addition to preformed LUV, lipid flip-flop is anticipated to accommodate cytochrome b_5 insertion into the vesicles' outer leaflet. This is qualitatively consistent with a cytochrome b_5 tight binding requirement of several hours and a DMPC flip-flop rate constant, k, of ~0.07 h^{-1} at 30°C (de Kruijff and van Zoelen, 1978).

Weiner and White (1991) give an excellent description of the three types of sample disorder: thermal, lattice and orientational, that will ultimately effect x-ray diffraction resolution limits. Thermal disorder would result in a decreased number of observed reflections due to increased atomic vibrational oscillation. Our cytochrome b_5:DMPC diffraction data were collected at 25.3°C which is slightly above the midpoint of the thermal phase transition (see Fig. 8) and would effect the relative amount of anticipated thermal disorder. The extent of thermal disorder in this system can be gauged by acyl chain packing character as shown in Fig. 7. Under these diffraction conditions, the average acyl chain packing vector is 4.45 Å with a reasonably sharp distribution envelope of ±0.31 Å (data not shown). The extent of system lattice disorder can be gauged by deconvoluting the beam width from the reflections to observe $1/e$ width changes as a function of reciprocal space coordinate (Blaurock, 1982). Examination of both film (see Fig. 2 *a*) and detector data reveals little change in the $1/e$ width as a function of s, consistent with the lack of significant lattice disorder. We have calculated, using the formulation of Wiener and White (1991), the max number of observable reflections, h_{max}, from our highest resolution data set to be 30 which is in reasonable agreement with the observed maximum of 27 reflections (see Fig. 2 *b*). The predicted h_{max} for lower resolution data sets (higher hydration, increased thermal and orientational disorder) are equally consistent with the numbers of observed reflections. As a result, we are confident that our thermally disordered structure is fully resolved (Wiener and White, 1991).

Figure 2 is representative of lamellar scatter obtained from the reconstituted cytochrome b_5:DMPC multilayer system. The film pattern shown in Fig. 2 *a* is $I_{exp}(s)$ obtained at 90% relative humidity and a repeat of 176.3 Å. Fig. 2 *b* represents the film data from a sample equilibrated to 84% relative humidity and 170.1 Å repeat. These two film patterns illustrate the trend in the intensity function as the structure factor is sampled at different unit cell repeats (see also Fig. 3). Note, for instance, the characteristic intensities observed for h = 9/10 and 12/13 in Fig. 2 *a*, where $h = 2\,d \sin\theta$. As the repeat spacing decreases, the h = 10 and 13 reflections become much weaker with concomitant increases in the h = 9 and 12 reflections. This is not unexpected because reflections (3, 6, 9) arise primarily from the lipid bilayer. In addition, note that the intensity between the second, third and fourth order reflections does not return to baseline. Since, as stated above, there is no significant lattice disorder, this observation is consistent with a double membrane unit cell and demands that these reflections share the same phase (Franks and Levine, 1981). A similar deduction could be made for the h = 9/10 and 12/13.

Typically, mosaic spread observed with these samples varies significantly as a function of multilayer hydration and ranges between 30–40° (Fig. 2 *a*) at high hydration to <17° (Fig. 2 *b*) as bilayers are dehydrated to lower water content. As the mosaic spread increases the intensity of the higher angle reflections are underestimated since the finite detector window precludes capture of the entire reflection. Furthermore, this effect is not constant (although it can be predicted given the sample mosaic spread, specimen to detector distance, window height and beam shape).

We arrived at an appropriate correction map by

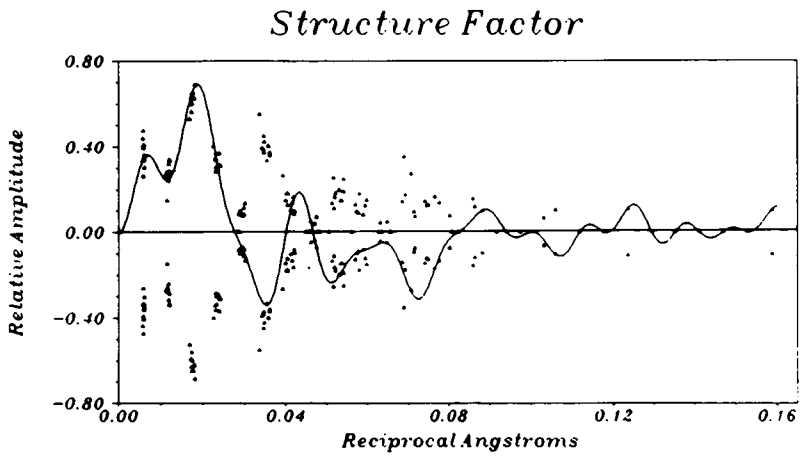

FIGURE 3 Structure factor plot generated from the correct lamellar intensity functions obtained from asymmetrically reconstituted cytochrome b_5:DMPC multibilayer samples at different repeat spacings (▲). The solid line represents the calculated structure factor from the fully resolved high resolution structure presented in Fig. 6.

comparing 1-dimensional laser densitometry data corrected for mosaic spread by [2 sin θ/λ] with detector data (from the same sample) s corrected incrementally between [2 sin $\theta/\lambda]^{0-1.0}$. Both sets of intensity data were initially Lorentz corrected by s. In addition, these intensity data were compared with detector data taken at shorter sample:detector distances where more reflections would be completely captured by the finite detector window. In essence, we applied geometric corrections to each reflection as a function of these parameters. This resultant $I_{cor}(s)$ (Fig. 2 *c* and Table 1) was in reasonable agreement with the 1-dimensional densitometry data. While higher angle reflections were clearly present in the film patterns (Fig. 2 *b*), we have generally been unable to observe $h \geq 18$ on our PSD due to detector signal to noise limitations. Therefore, structure factor amplitude values used to determine the fully resolved high resolution structure involves the combined use of both detector and film data where peak intensities common to both media were used for normalization. Intensity values for $h = 18$, 21 and 27 were difficult to evaluate accurately due to the steep background of the first film in the film stack (Fig. 2 *b, film a*). As such, these reflections could be over or under corrected in the final correct intensity function.

The process of phase determination followed essentially four approaches (Franks and Levine, 1981): swelling analysis (SF, Franks and Lieb, 1979), Patterson deconvolution (PD, Franks and Levine, 1981, Skita et al., 1986*a, b*), membrane model predictions (MM, Worthington, 1969) and pattern recognition (Luzzatti et al., 1972, Worthington and Khare, 1978). The structure factor amplitudes and phase assignments for some representative samples are shown in Table 1. Please note, we use "positive" to denote a phase of zero radians and "negative" to denote a phase of π radians. This table also contains phase assignments obtained on cytochrome b_5:eggPC system by Rzepecki and coworkers (1986).

The Shannon sampling theorem (Moody, 1963) was used, in the limit of assumptions, to confirm low resolution phase choices. This procedure (for recent discussion, see Young et al., 1991) involves generating a continuous Fourier transform from the derived $\rho_{exp}(z)$, sampling the transform at a different repeat unit and back transforming to generate a sampled $\rho_{sam}(z)$. This $\rho_{sam}(z)$ is then compared against a $\rho_{exp}(z)$ of the second repeat. Superposition of these two $\rho(z)$ demonstrates that the low resolution structure factors being sampled are the same (implicit assumption in this method) and confirms the phase choices. We call this method "swell check." There are two major limitations with respect to this approach. First, because we have a double membrane unit cell, swelling in the inner water space will alter the scattering element in the center of the unit cell and not just at the edges. This will alter, significantly, the structure factor as a function of hydration. Second, from the very assumption that the structure does not change as a result of hydration state, this method is limited to low resolution.

Fig. 3 illustrates the structure factor plot generated by changing multilayer hydration and, thereby sampling the continuous factor at discrete intervals in reciprocal space. It is not clear from the structure factor plot alone whether $h = 1$ is either positive or negative. Insight into the phase assignment for this particular reflection (quite important to the extent of bilayer asymmetry) was obtained by Patterson deconvolution (Fig. 4; Skita et al.,

TABLE 1 **Background and S corrected intensities for representative DMPC/b_5 multibilayers evaluated at different repeat spacings**

	$d1$	$d2$	$d3$	Phase assignments[δ]				
h	175.7 ± .5	173.7 ± .2	170.1 ± .6	α	SF	PD	MM	R*
1	5087	4161	3141	+	+	+	+	+
2	2089	1958	1608	+	+	+	+	+
3	9406	11380	11714	+	+	+	+	+
4	3114	2432	2362	+	+	+	+	+
5	190	268	158	—	—	—	—	0
6	4081	3723	3074	—	—	+	—	—
7	575	420	289	+	±	+	—	0
8	0	0	42	—	—	+	—	—
9	479	727	1095	—	—	+	—	—
10	437	215	188	—	—	—	—	—
11	0	0	70	—	—		0	0
12	530	815	2046	—	—		—	±
13	569	434	772	—			+	
14	—	0	0	0			0	
15	—	375	274	+			+	
16	—	—	0	0				
17	—	—	0	0				
18	—	—	291	—				
19	—	—	0	0				
20	—	—	0	0				
21	—	—	323	+				
22	—	—	0	0				
23	—	—	0	0				
24	—	—	0	0				
25	—	—	0	0				
26	—	—	0	0				
27	—	—	289	+				

α represents the phase set used in fully resolved high resolution electron density profile structure determination.

[δ]Phase assignment, α, generated from structure factor plot, SF; Patterson deconvolution, PD; membrane model, MM (Fig. 5), and comparison with literature value, R (Rzepecki et al., 1986). *Data from Rzepecki et al. (1986) was $d/2$ shifted to obtain structure shown in manuscript.

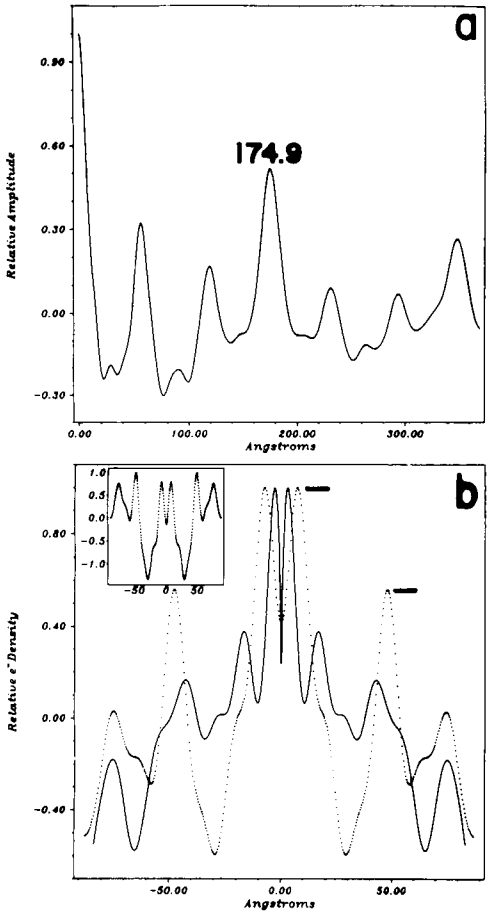

FIGURE 4 (*a*) Two unit cells of the multilayer Patterson function, $P_{ml}(z)$, derived from asymmetrically reconstituted cytochrome b_5/DMPC scattering data. Unit cell repeat for this sample is 174.93 Å. (*b*) Deconvolution result (——) obtained by direct deconvolution of unit cell Patterson, $P_{uc}(z)$. The deconvolution was performed from 174.93 Å $< x <$ 0.0 Å and the results mirrored about the origin. The method assumes a centrosymmetric unit cell. Included in this figure, is the $\rho_{exp}(z)$ (· · · ·) to illustrate the feature correlations between the deconvolution product and $\rho(z)$. The inset illustrates the $\rho(z)$ result obtained when the phase of the first order maxima is negative. Note the arrows which highlight inner and outer phospholipid headgroup (a)symmetry at $|z|$ = 7.6 and $|z|$ = 48.0 Å, respectively.

1986*a*, *b*). Fig. 4 *a* represents approximately two unit cells of the multilayer Patterson function obtained from a more highly hydrated and, therefore, more thermally disordered sample (for representative diffraction pattern, see Fig. 2 *a*). In this approach, which requires an effective finite sample size, we can calculate an electron density profile without an a priori knowledge of the phases (Fig. 4 *b*). We calculated $\rho(z)$ by deconvoluting the multilayer Patterson function, $P_{ml}(z)$, to obtain the unit cell Patterson which was further deconvoluted to obtain $\rho_{dcon}(z)$. The higher resolution information in $\rho_{dcon}(z)$ from this method is clearly in error, however, the general features and form of $\rho_{dcon}(z)$ (i.e., low resolution information) is very reasonable. This is evident in Fig. 4 *b* where the $\rho_{dcon}(z)$ is superimposed over the fully resolved low resolution structure (*dotted line*). Therefore, we expect that sampling a structure factor obtained by Fourier transform of $\rho_{dcon}(z)$ would yield accurate phase information for the low angle data ($s < 0.03$) and would most likely fail for higher angle reflections. In evaluating $\rho_{dcon}(z)$ for several samples, we found that the phases of the first four orders were positive and resulted in an asymmetric distribution of the phospholipid headgroup amplitudes at $|z|$ = 48 and 7.6 Å for the $\rho_{exp}(z)$ and 45 and 3.2 Å for the $\rho_{dcon}(z)$. The inset to Fig. 4 *b* illustrates the $\rho(z)$ obtained with a negative first order phase and demonstrates a lack of bilayer asymmetry resulting from this phase change. Thus, we were able to

unambiguously obtain the phase for the first order diffraction maxima by this method.

As stated previously, the fact that the intensity function between the second through fourth reflections (Fig. 2) does not return to background requires that these reflections share the same phase. In concert with the structure factor plot and first order phase predictions, this observation is compelling evidence for the phases of h = 2–4 being positive. The phase construction of the next two phases (h = 5, 6) is determined because h = 5 appears to be near a node, suggesting a phase change. Because h = 8 also appears to be at a node, we would predict an additional phase change for h = 8–10. A positive ninth order results in a structure which lacks a water space between the inner two headgroups (centered at $|z|$ = 6 Å in Fig. 6) in the centrosymmetric double membrane unit cell. This is a physically unreasonable phase choice given the nature of our hydrated multilayers. The model building approach (Fig. 5) predicts a negative ninth order which is also consistent with the assignment obtained by Rzepecki et al. (1986). As stated previously for h = 2–4, the nonzero background between h = 9/10 and 12/13 requires that h = 10 be negative.

Application of swell check to these partially resolved low resolution structures demonstrates that the $\rho_{sam}(z)$ is consistent with the $\rho_{exp}(z)$ only for h = 12, 13 having a negative phase. Because this is true, we can be confident of the phase assignments up to h = 13 for low resolution structures. Phases for the higher resolution structures are discussed below. Note in Table 1 that the phase construction, R, obtained for the eggPC:reconstituted cytochrome b_5 system is essentially the same as that derived for the DMPC:cytochrome b_5 system.

The electron density profiles for both the DMPC and heme peptide crystal structures (Pearson and Pascher, 1979 and Mathews et al., 1979, respectively) as oriented in Fig. 5 *a* were determined by summing the total number of electrons for each atom onto the z-axis ($\rho(z)$) where the volume element was defined by a Gaussian distribution with the full width at half maximum equal to the atomic van der Waals radii (Blechner et al., 1991). The resulting profiles (Fig. 5 *a*) are an atomic resolution picture of the input symmetric bilayer and oriented heme peptide structures. The lipid and protein electron density profiles (Fig. 5 *a*) were combined with protein: lipid ratio (1:30), the appropriate bilayer asymmetry as shown in experimental low resolution $\rho(z)$, repeat unit, and autocorrelation vector map to generate the strip function model shown in Fig. 5 *b*. The Fourier transform of this model yielded the structure factor shown in Fig. 5 *c* which was used to generate a set of phases for evaluation. The phase assignments obtained through this modelling approach are reasonably consistent with the phase set determined by Rzepecki et al. (1986) and those derived by our evaluation of the structure factor plot (Fig. 3).

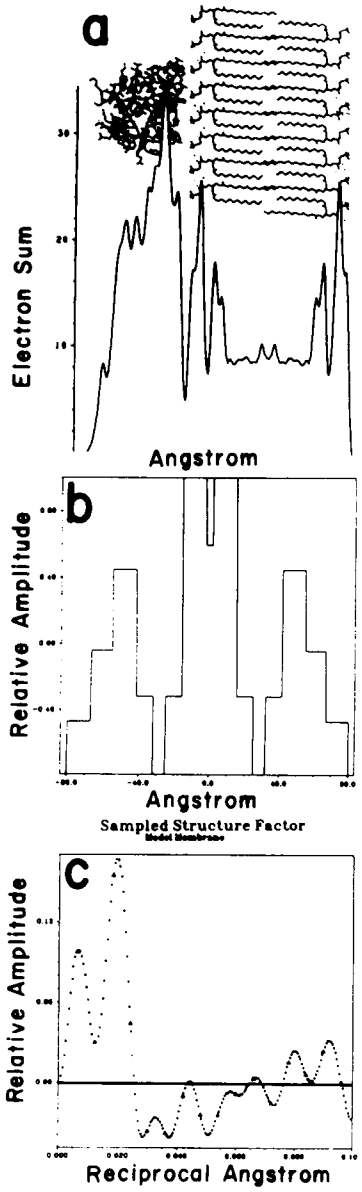

FIGURE 5 Smart model building for the purpose of initial phase prediction. Model parameters were derived from the combined use of crystal structure data and physical chemical data. (*a*) represents the $\rho(z)$ obtained by summing electrons from lipid and cytochrome b_5 crystal structures onto the z-axis. (*b*) represents a box model (d = 174.0 Å) derived from the $\rho(z)$, vector map derived from $P_{uc}(z)$ and physical chemical data; and (*c*) represents the Fourier transform of this model. Note that the amplitudes for h = 7 (s = .04) and 12 (s = .069) are close to a node and, therefore, determining the phase of these orders using this approach is difficult.

Phasing of the higher angle lamellar reflections was accomplished essentially by pattern recognition where

structural features observed in the partially resolved or fully resolved low resolution structures were maintained. Additionally, there is a limited number of potential phase choices for $h = 18$, 21, and 27. One complication to phasing the higher angle reflections is that, as the multibilayers are sequentially dehydrated, the protein structure at the edges of the unit cell begins to show some change. While McIntosh and Simon (1986) have found that the bilayer is relatively uneffected by dehydration induced compression, protein extending from the bilayer surface would be expected to exhibit some compressibility. The phase choices, α, shown in Table 1 for the fully resolved high resolution structure yield a $\rho(z)$ which directly superimposes upon the fully resolved low resolution structure. In addition, when the fully resolved high resolution $\rho(z)$ was thermally disordered by convolution with an 8 Å (FWHM) Gaussian, the resultant fully resolved low resolution structure gave good agreement with the fully resolved experimental low resolution structure. While global application of a thermal disorder factor would cause a uniform disordering of the entire bilayer, the result tends to confirm the phase assignments used to derive the high resolution structure.

Fig. 6 represents the fully resolved high resolution profile structure derived for this asymmetrically reconstituted DMPC:cytochrome b_5 system. This structure has several interesting features. First, it is clear that the membrane is structurally asymmetric. While more highly resolved, this bilayer asymmetry is similar to that observed by Rzepecki et al. (1986). In addition, the outer leaflet headgroups centered at $|z| = 48$ Å are broader than the inner leaflet headgroups (centered at $|z| = 6$ Å) consistent with protein penetration through this portion of the membrane. The heme peptide portion of the membrane structure, located at the edges of the double membrane unit cell ($|z| = 55 - 85$ Å), contribute several peaks of electron density. Based on modeling data to be presented in the Discussion, there is reason to believe that the heme peptide has a preferential orienta-

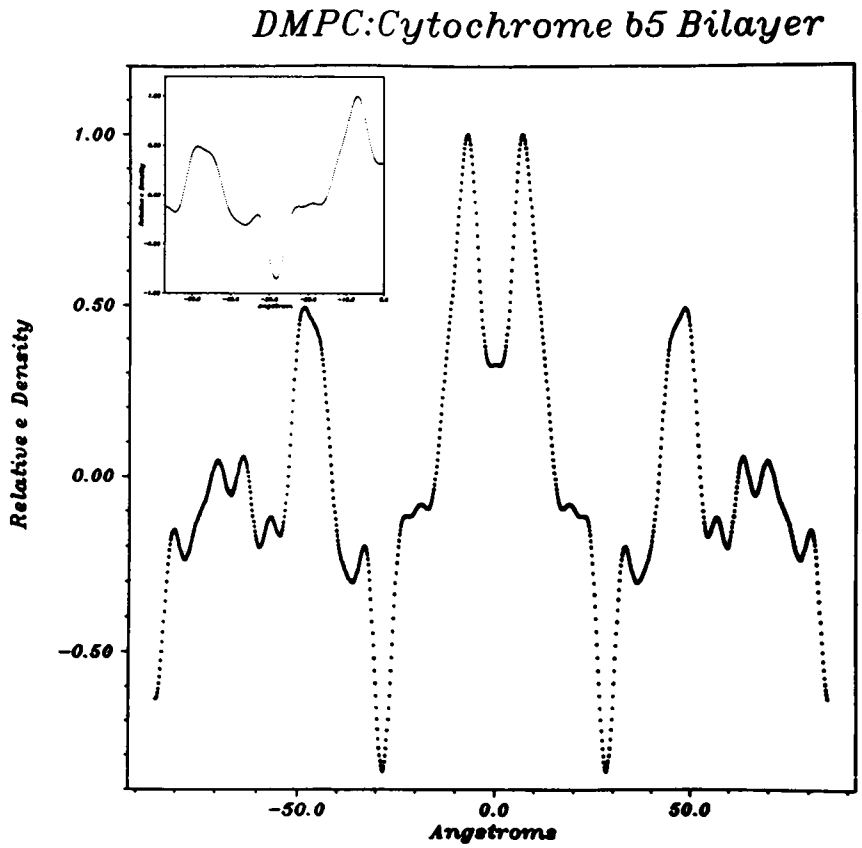

FIGURE 6 Final experimental electron density profile structure derived for the asymmetrically reconstituted cytochrome b_5:DMPC bilayer at 6.3 Å resolution. The phase and intensity data used in calculating $\rho(z)$ are shown in Table 1. The slight rippling between the inner water space and inner methyl region of the bilayers is due to scanning densitometry integration error for the high angle reflections due to a steep background (Fig. 2 *b*). Decreasing the amplitude of $h = 27$ by ~50% completely abrogates these ripples without changing appreciably the rest of the profile structure. The inset highlights the bilayer portion of the profile structure such that the structural asymmetry can be appreciated.

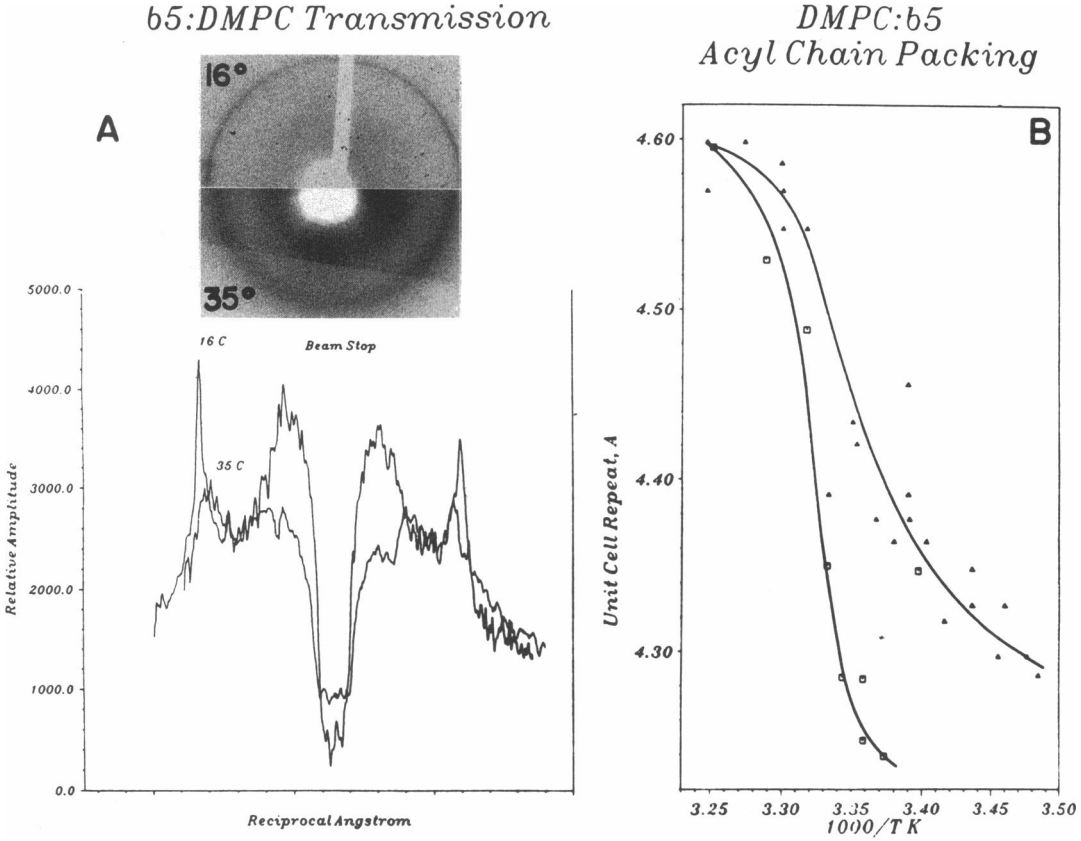

FIGURE 7 (*a*) Represents x-ray transmission scattering profiles derived from multilayer samples oriented perpendicular to the incident beam. The upper panel represents film pattern for sample at 16°C and a quasihexagonal acyl chain packing lattice whereas the lower panel represents the disordered acyl chain packing observed at 35°C. Below is a densitometry scan along the film fiducial. (*b*) Acyl chain packing repeat spacing as a function of reciprocal temperature, K. for pure DMPC (□) and asymmetrically reconstituted cytochrome b_5/DMPC bilayers at a lipid/protein ratio of 1:32 (△).

tion with the heme plane perpendicular to the bilayer normal. Fig. 5 *a* and Fig. 10 *a*, *c–e* illustrate that the $\rho(z)$ of the heme peptide in this orientation would produce electron density profile features associated with both the heme/Fe^{2+} porphyrin ring and α-helical peptide constituents. Other pertinent features common to double membrane systems are the inner water space centered at $x = 0$ Å, the methyl trough centered at $|z| = 28$ Å, and the inner and outer acyl chain regions centered at $|z| =$ 19 and 35 Å, respectively. Lastly, there is a peak in the electron density profile located approximately 20 Å from the outer leaflet headgroup (see *inset, arrows*). This peak falls at precisely the location determined for tryptophan 109 by Fleming and co-workers (1979). This peak in the electron density profile could result from the stacked tryptophan 108/112 rings oriented perpendicular to the bilayer normal. While there is marked structural perturbation in the membrane outer leaflets (centered around $|z| = 35$ Å), The inner leaflet acyl chain regions (centered around $|z| = 18$ Å) appears to be relatively unperturbed by the presence of asymmetrically reconstituted cytochrome b_5. We, therefore, have interpreted this cytochrome b_5:DMPC membrane structure to be consistent with a *cis* NPP configuration in which the NPP does not penetrate appreciably beyond the bilayer midplane.

Transmission x-ray studies were performed to evaluate thermotropic dependence of acyl chain packing as a function of asymmetric protein incorporation. In addition, coherently scattering α-helical protein segments oriented parallel to the bilayer normal would potentially be observed as reflections occurring at 1/10 Å (Blaurock, 1975, Herbette et al., 1977).

These data are shown in Fig. 7. As stated in the Methods, transmissions studies were carried out by placing the samples on 'slotted EM grids' that had been coated with a 30–60 nm 'Butvar' coat. Fig. 7 *a* represents transmission x-ray scattering patterns from DMPC control multibilayer samples at 16 (*top*) and 35°C (*bottom*). A densitometry tracing along the fiducial is presented below and the calculated acyl chain packing repeat

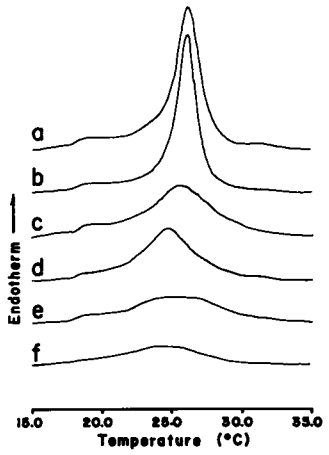

FIGURE 8 Differential scanning calorimetry studies performed on control DMPC membranes (*a*, *b*) and DMPC membranes asymmetrically reconstituted with either 1:78 (*c*, *d*) or 1:32 (*e*, *f*) cytochrome b_5/lipid ratio. In each condition, fully hydrated (*a*, *c*, *e*) and partially hydrated (*b*, *d*, *f*) thermograms are presented. Samples were maintained at 4°C following encapsulation to maintain a constant initial thermal history. See text for transition temperatures and enthalpy data.

spacings as a function of temperature are shown in Fig. 7 *b*.

Fig. 7 *b* illustrates that the DMPC:cytochrome b_5 acyl chain packing transition from 4.65 Å to 4.26 Å occurs over a broad temperature range centered at ~25°C. This transition temperature is similar to the t_m observed in both calorimetric and fluorescence anisotropy studies shown in Figs. 8 and 9, respectively. The low temperature 4.26 Å acyl chain packing in these reconstituted membrane multilayers is consistent with a quasihexagonal acyl chain packing lattice which, in some way, must accommodate the presence of surface saturating concentrations of cytochrome b_5. In the control DMPC multilayer experiments shown in Fig. 7 *b*, the transition is sharp and exhibits a midpoint at approximately 26°C consistent with calorimetrically observed t_m. Thermotropic changes in acyl chain packing for both the reconstituted cytochrome b_5/DMPC and pure DMPC bilayers can be ascertained from changes in both the width and radius of the transmission ring. For cytochrome b_5/DMPC and pure DMPC bilayers, changes in these parameters from 4.57 ± 0.44 Å to 4.29 ± 0.07 Å and 4.60 ± 0.34 Å to 4.24 ± 0.04 Å, respectively (data not shown), correlate to smooth thermal transitions from 5 to 40°C. Note that the diffraction studies were performed at a temperature of 25.3°C (midpoint of the thermal phase transition) such that the membrane acyl chain packing parameters were 4.45 ± .22 Å at 90% relative humidity.

Because these transmission scattering experiments were performed statically, two important factors, bilayer stability and transition kinetics, have to be kept in mind. We have demonstrated stability in both multibilayer repeat spacing and reconstitution asymmetry. Therefore, the only thermally inducible transition would involve lateral segregation of peptide and resultant changes in acyl chain packing. In these experiments, the vesicles were reconstituted with surface saturating concentrations of cytochrome b_5, thereby, limiting the potential for lateral protein diffusion. We have noted in lamellar scattering studies, however, that we could thermotropically induce a reversible transition in the single domain ~168 Å repeat membranes to a pure DMPC (~58 Å) domain and a slightly larger DMPC: cytochrome b_5 (~186 Å) domain. This observation is consistent with an alteration in heme peptide orientation and, hence, cytochrome b_5 packing because the change in the large unit cell could be accounted for strictly by the axial ratio of the oblate ellipsoid heme peptide. The kinetics of this type of a transition appear to be reasonably rapid. In one experiment, we 'watched' the transition occur over approximately 1 min of 2°C temperature elevation during lamellar data collection. While qualitative, this observation suggests that the 15–20 min equilibration time at each temperature should be sufficient for thermal stabilization.

A third consideration involves the temperature dependence of sample relative humidity as modulated by saturated salt solutions. While we have not directly measured this lyotropic effect, the temperature coefficient for the saturated $ZnSO_4 \cdot 7\ H_2O$ is such that the relative humidity increases by ~4.5 percent on moving from 20 (90%) to 5°C (94.5%). As such, this slight thermotropic effect on the relative humidity would actually tend to decrease bilayer compression and limit acyl chain condensation as a strict function of hydration force.

Transmission x-ray studies would reveal the presence of coherently scattering α-helical segments oriented parallel with the bilayer normal (Blaurock, 1975, Herbette et al., 1977). We found no evidence of any reflection in the 1/10 Å region suggesting that there is no coherently scattering α-helical element of significant size in these membranes. This observation has particular significance with respect to a trans NPP configuration that would be anticipated to have significant α-helical content. Because each centrosymmetric double membrane unit is saturated with cytochrome b_5 (consider effect of flattening a vesicle with its surface saturated with protein), we would anticipate that a structural scattering element, such as an α-helical peptide, would be a regularly repeating and, therefore, observable with this type of diffraction geometry. As such, this finding is

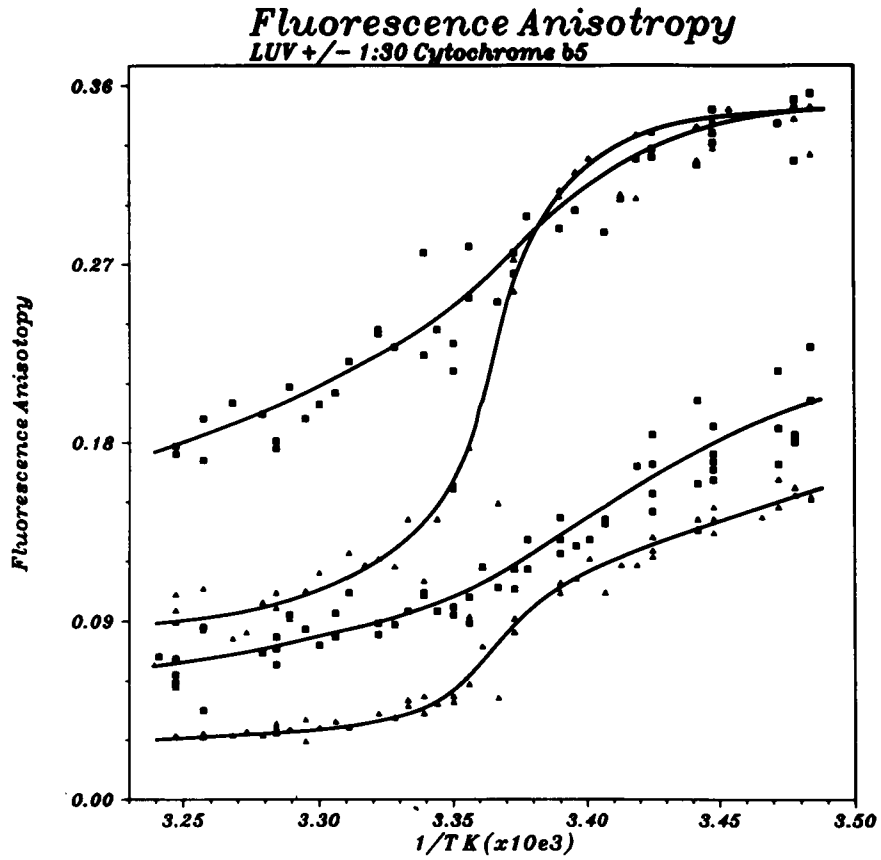

FIGURE 9 Temperature dependent fluorescence anisotropy data for the probes Diphenylhexatriene (*upper two curves*) and perylene (*lower two curves*) incorporated into DMPC LUV in the presence (□) and absence (▲) of 1:32 cytochrome b_5. Plot represents a scatter plot of data from a number of experimental runs. All data were collected from 100 μM vesicle phosphate.

inconsistent with significant α-helical segments aligned along the bilayer normal.

DSC and fluorescence anisotropy measurements were carried out to evaluate the reconstituted bilayer physical dynamics as a means of constraining our interpretation of the structural data. Additionally, these studies would allow us to more fully understand the peptide/lipid interaction. The dsc results on the asymmetrically reconstituted 800–1,000 Å cytochrome b_5/DMPC vesicles are shown in Fig 8 in which two sample conditions are presented: fully hydrated LUV and partially dehydrated (90% relative humidity) multilayer stacks. Control DMPC LUVs had t_m values of 26.3 and 25.8°C for the fully (Fig. 8 *a*) and partially (Fig. 8 *b*) hydrated membranes, respectively. The transition enthalpies for both samples were 38.73 *J/g* (6.28 Kcal/mol) and were not significantly different than the values obtained for the fully hydrated multilamellar vesicles and partially hydrated multibilayer membranes of 34.66 ± 7.7 *J/g* (6.1 Kcal/Mol) and 40.41 ± 3.4 *J/g* (7.09 Kcal/Mol), respectively. Note the presence of a small enthalpic pretransition of ~0.73 *J/g* (0.12 Kcal/Mol) in both the fully and partially hydrated samples. The $\Delta t_{1/2}$, an estimate of the transition cooperative unit size, is approximately equal in both cases with a value of 1.4 ± 0.2°C.

The asymmetric reconstitution of cytochrome b_5 into DMPC LUV at 1:78 (Fig. 8 *c, d*) and 1:29 (Fig. 8, *e, f*) mole ratio clearly decreases the transition enthalpy, broadens the transition, while the t_m remained essentially unchanged. The transition enthalpies for the 1:78 and 1:29 ratio reconstituted fully hydrated LUV bilayers (Fig. 8 *c, e*) were 23.43 *J/g* (6.01 Kcal/Mol) and 12.42 *J/g* (4.26 Kcal/Mol), respectively. A similar range of values were observed for the partially hydrated multilayer samples. In both cases the $\Delta t_{1/2}$ value increased precipitously as a function of increasing protein:lipid ratio. A plot of $\Delta H/\Delta H_0$ vs protein/lipid ratio demonstrated that ~10–16 lipid molecules are removed from the cooperative unit by asymmetric cytochrome b_5 reconstitution (data not shown). Both onset (t_l) and upper limit (t_h)

temperatures were dramatically effected by asymmetric protein incorporation. Note, however, that the pretransition evident in the pure DMPC bilayers was observed in the reconstituted membrane preparations even at surface saturating cytochrome b_5 concentrations. This is particularly obvious in the fully hydrated samples (Fig. 8, *a*, *c*, *e*). In dsc studies focused on the bilayer interaction of both the bee venom, Melittin (Mollay, 1972), and Ca^{+2}, Mg^{+2}-ATPase (Gomez-Fernandez et al., 1980), the pretransition was removed at reasonably low protein/lipid ratios (ranging from 1:153, 250 for the ATPase and Melittin, respectively). In addition, Mollay (1972) determined the hydrophobic segment was responsible for the decrease in the pretransition. Our thermograms demonstrate that there is an approximate 32% decrease in pretransition enthalpy as a result of asymmetric cytochrome b_5 vesicle reconstitution. Were the NPP to be transmembrane, Mollays' (1972) data would predict complete abrogation of the pretransition. It is reasonable, then, to suggest that the observed decrease in DMPC pretransition by less than 50% represents further corroborative evidence for the fact that the NPP does not perturb both leaflets of the membrane in this asymmetrically reconstituted system.

An interesting feature of these transitions is the observation that the t_h is moved to higher temperature in the asymmetrically reconstituted samples. This observation is similar to that reported for several peptides in a review by McElhaney (1986). As such, a fraction of the bilayer lipid is melting at higher temperature. This fraction may be related to that cooperative unit of lipid directly adjacent to the protein (George et al., 1990). Dehlinger and co-workers (1974) have demonstrated using ESR spin probe analysis that there is a segment of immobilized lipid in the presence of cytochrome b_5.

The temperature dependence of diphenylhexatriene (DPH) and perylene fluorescence anisotropy in control and asymmetrically reconstituted cytochrome b_5:DMPC vesicles is shown in Fig. 9. In these experiments, the probes were preincubated with the DMPC LUV membranes before reconstitution to minimize the potential that the probe could be interacting with the heme peptide moiety. Experiments in which the probes were added directly to the reconstituted membrane yielded essentially the same results suggesting that the probes were reporting on their bilayer location rather than any preferential interaction with the protein. Under the experimental conditions imposed, probe to lipid ratios were maintained at or below a 1:1000 ratio with a constant 1:30 protein:lipid ratio for the reconstituted bilayers. The data shown in Fig. 9 clearly indicate that under essentially all conditions, the asymmetrically reconstituted cytochrome b_5:DMPC bilayers are more 'crystalline' than the membranes in the absence of peptide. Because these probes are traditionally considered to be reporting from the hydrocarbon core of the membrane, these data are clearly consistent with the observation of protein mediated acyl chain immobilization. This observation is consistent with that of Williams and co-workers (1972) and Verma et al. (1974) who have observed increased fatty acyl chain segmental disorder and decreased fluidity in reconstituted melittin bilayers, the disparity being attributed to acyl chain:peptide interactions.

DISCUSSION

These studies were designed to determine the fully resolved high resolution structure of the asymmetrically reconstituted cytochrome b_5:DMPC bilayer. In addition, we wished to obtain bilayer physical dynamics data which would serve the dual purpose of allowing us to constrain our structural models as well as begin to more fully appreciate the peptide:lipid interaction. This combined approach should aid our understanding of how this protein interacts with other membrane associated proteins. Cytochrome b_5 interaction with the transmembrane desaturase is of particular interest because the mechanisms involved in the transfer of reducing potential between the heme peptide and the desaturase non-heme iron remains unclear. The interaction between cytochrome b_5 reductase and cytochrome b_5 has been demonstrated by Strittmatter et al. (1990) to extremely stereospecific with direct association between the cytochrome b_5 heme propionyl carboxyl groups and lysine residues on the reductase flavopeptide. We would predict, based on the stereochemistry of this peptide interaction during electron transfer, that the cytochrome b_5:desaturase interaction would be equally stereochemically constrained.

The relative electron density profiles shown in Figs. 6 and 10*f* reveal four basic features: (*a*) asymmetry in the bilayer headgroup peaks; (*b*) the apparently unperturbed inner leaflet acyl chain region; (*c*) the increased electron density in the outer leaflet which we have interpreted as stacked tryptophan rings; and (*d*) the electron density associated with the heme peptide. We have interpreted this structure not only to be consistent with a *cis* cytochrome b_5 configuration in which the NPP penetrates to approximately the bilayer midplane, but, inconsistent with the *trans* interpretation. Additional evidence was obtained from the calorimetry studies in which we observed a pretransition even under the

conditions of cytochrome b_5 surface saturation. As discussed previously, penetration of nonpolar portions of peptides (e.g., Melittin) into bilayers at very low protein:lipid ratios abrogates the pretransition completely. The increased fluorescence anisotropy in asymmetrically reconstituted cytochrome b_5 vesicles is also consistent with this interpretation.

Evaluation of peptide contributions to different regions of a model structure would assist us in establishing the sensitivity of the model to different NPP configurations. We must state at the outset that we are not ascribing, a priori, a specific secondary structure to the NPP but, rather, attempting to constrain models to currently available physical/chemical data. These data include: the primary NPP amino acid sequence, NPP molecular volume, location of Trp 109 determined by resonance energy transfer experiments (Fleming et al., 1979), Tyr 129 availability for pH titration (Dailey and Strittmatter, 1981), apparent stacking of Trp residues 108 and 112 (Strittmatter and Dailey, 1982), protease accessibility of carboxyl- (Ozols, 1989) and amino- (Strittmatter et al., 1972) terminal residues, experimentally determined lipid/protein ratios, and bilayer dimensions. In addition, we have attempted to incorporate previously predicted NPP secondary structural features (Strittmatter et al., 1972, Strittmatter and Rogers, 1982, Holloway and Bucheit, 1990). Using these constraints, we have built three different structural variations: *trans* configuration composed of primarily α-helical segments with random or extended regions at the carboxyl- and amino-termini, *cis* model comprised of α-helical intrabilayer sequences and a *cis* model containing a mixture of antiparallel β-sheet, 3/10 helix, α-helix, and β-turn as proposed by Strittmatter and Dailey (1982). Once assembled these NPP molecules were ligated to the heme peptide which was oriented with the heme plane parallel to the bilayer as suggested by Mathews (1979) and illustrated in Fig. 5 *a*.

The results of the ρ(*z*) model calculations are shown in Fig. 10. Fig. 10 *a* illustrates the ρ(*z*) for holocytochrome b_5 (no lipid) assuming an all α-helical NPP secondary structure. Note the predicted increase in electron density associated with the aromatic ring containing amino acids in the primary structure (located at approximately $|z| = 6$, 15, and 30 Å). On average, the electron density of an α-helical segment is reasonably uniform supporting the idea that a *trans* configuration would simply elevate the average bilayer electron density. The aromatic ring containing residues would tend to introduce modulations into the bilayer acyl chain and methyl trough region as illustrated in Fig. 10 *c*. In addition, note in Fig. 10 *a*, the heme peptide structural detail, particularly, the peaks associated with the heme group. If, in the context of a diffraction experiment, there were

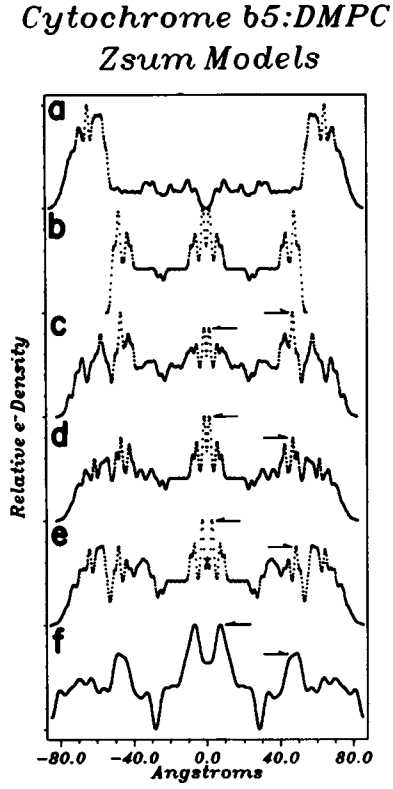

FIGURE 10 Model figures generated for evaluating the structural sensitivity to different NPP configurations across the DMPC membrane bilayer. In these models, crystal structure coordinates were used for both the heme peptide and DMPC. The NPP configurations were derived by generating *cis* or *trans* peptide segments from the NPP primary structure which, upon insertion into the model lipid, attempt to conform to physical chemical data (*a*) Cytochrome b_5 with NPP in fully *trans*, all α-helical configuration (no lipid component). (*b*) Double membrane of pure DMPC lipid. (*c*) Combined projection of a and b onto *z*-axis. (*d*) Cytochrome b_5 NPP segment comprised of ~60% α-helix and arranged in *cis* configuration. Ends of the NPP segment are in extended configuration and ascending/descending helical elements are hooked together by two β-turns. (*e*) represents a similar *cis* NPP configuration but contains the structural elements predicted by Strittmatter and Rogers (1982). (*f*) Experimental electron density profile shown in Fig. 6.

significant structural organization of these various regions of the cytochrome b_5 molecule in the membrane, projection onto the *z*-axis would allow us to identify, within resolution limits, the superposition of these structural elements in the final ρ(*z*). Disorder, on the other hand, would tend to abrogate these structural details.

In building the reconstituted protein models, lipid asymmetry as a consequence of asymmetric protein incorporation had to be considered. The lack of vesicle structural alterations (see Fig. 1) and the time dependence for stable (tight) cytochrome b_5 reconstitution

suggest that phospholipid flip-flop would be required to facilitate the reconstitution process. This asymmetry in bilayer lipid content has been observed in other systems (e.g., Herbette et al., 1985). With a starting protein:lipid ratio of 1:30, we can arbitrarily generate bilayer lipid asymmetry (the wonders of the computer age) and evaluate its impact on $\rho(z)$. These model profiles are shown in Fig. 10, *c–e*. The phospholipid headgroup asymmetry has been highlighted by lines drawn to the peak height to aid interpretation. Fig. 10 *c* represents the *trans* NPP model incorporated into the DMPC membrane illustrated in Fig. 10 *b*. In this structure, the carboxyl- and amino-terminal segments have been given extended structures to preserve the relative location of tryptophan 109 along the bilayer normal (in this case, 16 Å from the edge of the bilayer) and the carboxyl-terminal residue accessibility to proteolytic cleavage demonstrated by Ozols (1989). The phospholipid profile has been maintained symmetric, in this Figure, because it is assumed that the α-helical peptide sequence would occupy similar areas in both leaflets. Beyond the imposed symmetry in the headgroup amplitudes, note that there is significant perturbation to both acyl chain regions of the bilayer. The slight decrease in the electron density of the inner leaflet phosphate headgroup density is due to the fact that, at 42 Å in length, the NPP cannot completely span through this region. This latter fact alone seriously limits the possibility of a transmembrane α-helical NPP configuration. Even at an α-helical content of approximately 60% (Holloway and Mantsch, 1989), there is not sufficient NPP length to cross the membrane bilayer and be consistent with the biochemical data. Additionally, the transmission x-ray studies failed to detect any coherently scattering α-helical segments parallel to the bilayer normal. When evaluated in light of the fully resolved high resolution structure shown in Fig. 10 *f* (and Fig. 6), this *trans* model does not adequately fit the experimentally derived data.

Fig. 10, *d* and *e* represent *cis* NPP configurations within the membrane bilayer. The NPP conformation in these two models differs in that Fig. 10 *d* is comprised of ascending and descending α-helical segments separated by essentially 2 β-turns while that in Fig. 10 *e* contains the predicted structural elements suggested by Strittmatter and Dailey (1982). In particular, the structure depicted in Fig. 10 *e* has antiparallel β-sheet structure traversing the headgroup region. This latter structure allows for increased peptide bulk closer to the center of the membrane bilayer. In both cases, these two models conform to the physical chemical data available for membrane bound cytochrome b_5. Because we predict that asymmetric reconstitution is facilitated by lipid flip-flop, we made the bilayers successively asymmetric in headgroup amplitude by flipping lipids into the inner leaflet. We needed to flip six and four lipids for the models shown in Fig. 10 *d* and *e*, respectively, to compensate for the volume occupied by the protein in the outer membrane leaflet. Assuming the NPP segment placement along the bilayer normal in these latter two structures is reasonable, these models would predict that the outer leaflet headgroup peak would be broadened by the presence of the aromatic rings associated with the tyrosine residues (126, 129) near the carboxyl terminus.

How do these models compare with the experimentally observed high resolution structure? Fig. 10 *f* is the fully resolved high resolution structure for the asymmetrically reconstituted cytochrome b_5:DMPC bilayer shown in Fig. 6. From a purely visual standpoint, there is strong structural similarity between the experimentally derived structure and that modelled in Fig. 10, *d* or *e*. The argument for the *cis* model is further strengthened by the fact that the Fourier transform of the model $\rho(z)$ yields a structure factor quite similar to that obtained experimentally.

These modeling results rule out an all α-helical NPP transmembrane segment on purely physical grounds, because none of the physical chemical parameters could be met by this type of configuration. These modeling results suggest that this asymmetrically reconstituted DMPC:cytochrome b_5 system should be quite sensitive to changes in peptide organization along the bilayer normal. Isomorphous replacement studies (either x-ray or neutron) would allow us to (*a*) place our profiles on an absolute electron density scale, and (*b*) demonstrate conclusively the NPP distribution within the bilayer structure. In addition, the recent report by Ladohkin et al. (1991) of a cloned rabbit cytochrome b_5 would significantly enhance the potential to ascertain the structural distribution of this peptide along the bilayer normal since specific isomorphous residues could be incorporated into the structure.

Fleming and co-workers (1979) have determined that tryptophan 109 is located at ~20 Å from the edge of the bilayer. Resonance energy transfer studies by Friere et al. (1983) also yield data consistent with this conclusion. Markellow et al. (1985) and Tennyson and Holloway (1986), on the other hand, have suggested from bromine lipid quenching studies that tryptophan 109 is located approximately 7 Å below the bilayer surface. It is interesting that a peak of electron density appears in the profile structure (Figs. 6 and 10 *f*) at ~20 Å into the bilayer, a position consistent with that location determined by Fleming et al. (1979). At this point, the origin of the discrepancy in tryptophan 109 location between Holloway and co-workers and these other reports is unclear. A plausible explanation may involve the method of reconstitution and/or mode of cytochrome b_5 inser-

tion into the membranes. One principle difference is that membranes prepared by Fleming et al. (1979) and in the current structure studies were comprised, principally, of DMPC in which tight cytochrome b_5 binding has been demonstrated to occur readily. It is interesting, as stated above, that Friere and co-workers (1983) identified a similar 20–22 Å tryptophan 109 location in DMPC membranes using resonance energy transfer between pyrenedecanoic acid and tryptophan 109. Markello et al. (1985) and Tennyson and Holloway (1986, 1991), on the other hand, used a palmitoyloleoylphosphatidylcholine (POPC) system. Enoch et al. (1979) have shown that tight cytochrome b_5 binding to egg phosphatidylcholine is rather constrained. In addition, studies designed to determine the detailed dioleoylphosphatidylcholine structure by Wiener and White (1991*b*) reveal that the bromine distribution in these membranes is quite large despite their specific labeling at the Δ9–10 methylene segments. Thus, a wider than anticipated bromine distribution in the POPC membranes used by Markello et al. (1985) and Tennyson and Holloway (1986) could cause additional uncertainty in the location of the bromine quenched tryptophan 109. The argument here is the traditional discussion between the point quencher versus a quencher that has some spatial distribution (Wiener and White, 1991*b*). As such, the discrepancy between our data on tryptophan 109 location and that of Tennyson and Holloway (1986) remains unresolved.

One interesting feature of the modeling are the peaks of electron density associated with the heme peptide. Mathews et al. (1979) suggested that the heme peptide may have a preferential orientation, with the heme plane perpendicular to the bilayer normal on association with the membrane. In an interesting series of studies, Pachence and co-workers (1990) have examined the bilayer surface orientation of cytochrome c using x-ray resonance at the heme iron absorption edge. In these studies, it was determined that the porphyrin ring structure of the cytochrome was oriented perpendicular to the bilayer normal. In a recent publication, Ozols (1989) has illustrated a random cytochrome b_5 heme peptide orientation with respect to the bilayer surface. In the interaction of cytochrome b_5 with both its reductase and the fatty acid desaturase, it seems reasonable that the heme peptide would have a preferential orientation dictated, to some extent, by the bilayer lipid composition. To evaluate this possibility, we examined the electric potential map of the heme peptide crystal structure (Mathews et al., 1979). Essentially, we examined the charge character of the 'underside' of the protein. The 'underside' is defined as the tertiary structure formed by the helical segments I, II, III, and VI illustrated in Mathews et al. (1979) and would be juxtaposed to the bilayer surface when the heme peptide is oriented as described above. Based on the charge characteristics of the amino acid residues, the CHEMX program calculates a surface electric potential map. The results indicate that there are two large regions of positive and negative surface charge potential which would tend to interact electrostatically with the phospholipid headgroups in the native membrane. Preliminary data has been obtained in which suberimidate was found to specifically crosslink lysine 28 (located on the underside of the heme peptide) and phosphatidylethanolamine added into large unilamellar vesicles (Rzepecki, unpublished observation). The latter is strong compelling evidence for a preferential orientation of this region of the peptide on the bilayer surface. Moreover, this would provide a 'stable' porphyrin ring orientation for efficient electron transfer.

Papahadjoupolos (1975) has postulated that specific peptide:bilayer interactions would yield specific effects upon the calorimetrically determined transitions in these membranes. Essentially, surface bound, electrostatically interacting peptides decrease the thermal phase transition and reduce the transition enthalpy. Peptides which partition into the bilayer, on the other hand, effect differentially the transition enthalpy and t_m. In some cases, the t_m has been shown to remain constant or even increased slightly by the insertion of certain peptides into the membrane bilayer (McElhaney, 1986). Cytochrome b_5 contains both peptide moieties: a soluble fragment that interacts electrostatically with the bilayer surface and the NPP which penetrates into the membrane hydrocarbon core. Initial calorimetry data on asymmetrically reconstituted cytochrome b_5 membranes demonstrate the anticipated decrease in enthalpy with increasing protein concentration. However, these calorimetry data demonstrate that the t_m remains essentially uneffected while the upper and lower limits are modulated by asymmetric peptide reconstitution. As stated in the Results section, the t_h in these membranes has been pushed to higher temperatures as a function of asymmetric incorporation of cytochrome b_5 into DMPC large unilamellar vesicles. Friere and co-workers (1986), in examining the thermotropic behavior of reconstituted DMPC:cytochrome b_5 vesicles did observe that the transition temperatures were relatively uneffected by the presence of peptide, while on the other hand, they did not observe a similar effect on t_h. In addition, the broadening of the transition was not nearly as marked as that observed in these studies. In contrast, our data clearly demonstrate that asymmetric reconstitution of cytochrome b_5 into the DMPC bilayer perturbs the cooperative behavior of the thermal phase transition. Friere et al. (1986) and Oldfield et al. (1978) suggest that the lipid removed from the cooperative thermal phase transition are conformationally disordered.

While, as demonstrated in Fig. 7, the average acyl chain packing is more disordered in the cytochrome b_5 reconstituted membranes, fluorescence anisotropy studies indicated that these same membrane preparations were substantially less fluid in the presence of surface saturating protein under all temperature conditions. The transmission x-ray scatter studies yield information about the in-plane packing density of acyl chains primarily from the upper chain region of the membrane lipid. The fluorescence probes, on the other hand, are traditionally assumed to be 'reporting' from the center of the bilayer. In the fluorescence experiments, two probes which differ in rotationally averaged structure were used to assess the bilayer physical dynamics. Taken together, these data suggest that there is an increased acyl chain segmental order parameter on approach to the center of the membrane. If this is correct, evaluation of the gauche-trans rotomer ratio in the presence and absence of cytochrome b_5 should give us some additional insight into the interaction dynamics between the lipid and peptide. One consideration for these types of studies, however, is that different samples (and, hence, potentially different sample conditions) must be used for separate studies. In a rather elegant set-up, Ungar and Feijoo (1990) combined calorimetry and x-ray scattering such that thermal and structural events could be monitored simultaneously and directly correlated. An approach of this type for lipid and lipid-protein complexes would substantially enhance our abilities to evaluate the complex transition behavior that occurs in these liquid crystalline systems.

In conclusion, we present a structure for the asymmetrically reconstituted cytochrome b_5:DMPC system at ~6 Å resolution. This structure demonstrates that the NPP moiety of cytochrome b_5 is oriented in a 'cis' configuration with the protein penetrating only to the bilayer midplane. In addition, this interpretation is consistent with both model predictions and physical dynamics studies.

The authors would like to acknowledge the technical assistance of Ms. B. Eydelshteyn. In addition, we would like to thank Dr. Mark Trumbore for his assistance with the molecular modeling aspects of this project. We would also like to acknowledge Mr. Richard Kelley whose tireless efforts maintained our computer systems in operational order. We would also like to acknowledge Drs. David Rhodes and Leo Herbette for insightful discussions of these data.

The CHEMX graphics package used for the molecular modeling section of this work was developed and distributed by Chemical Design, Ltd., Oxford, England. These studies were funded by National Institutes of Health grant GM-15924.

Received for publication 19 April 1991 and in final form 10 December 1991.

REFERENCES

Arinc, E., L. M. Rzepecki, and P. Strittmatter. 1987. Topography of the C terminus of cytochrome b_5 tightly bound to dimyristoylphosphatidylcholine vesicles. *J. Biol. Chem.* 262:15563–15567.

Blaurock, A. E. 1975. Bacteriorhodopsin: a transmembrane pump containing α-helix. *J. Mol. Biol.* 93:139–158.

Blaurock, A. E. 1982. Evidence of bilayer structure and of membrane interactions from x-ray diffraction analysis. *Biochim. Biophys. Acta.* 650:167–207.

Blechner, S., W. Morris, P. Schoen, P. Yager, and D. Rhodes. 1991. Structure of polymerizable lipid bilayers II: two heptacosadiynoyl phosphatidylcholine isomers. *Chem. Phys. Lipids.* 58:41–54.

Chester, D. W., L. G. Herbette, R. P. Mason, A. F. Joslyn, D. J. Triggle, and D. E. Koppel. 1986. Diffusion of dihydropyridine calcium channel antagonists in cardiac sarcolemmal lipid multibilayers. *Biophys. J.* 52:1021–1030.

Clark, N. A., K. J. Rothschild, D. A. Luippold, and B. A. Simon. 1980. Surface-induced lamellar orientation of multilamellar membrane arrays. Theoretical analysis and a new method with application to purple membrane fragments. *Biophys. J.* 31:65–96.

Dailey, H. A., and P. Strittmatter. 1978. Structural and functional properties of the membrane binding segment of cytochrome b_5. *J. Biol. Chem.* 253:8203–8209.

Dailey, H. A., and P. Strittmatter. 1981. Orientation of the carboxyl and NH_2 termini of the membrane-binding segment of cytochrome b_5 on the same side of phospholipid bilayers. *J. Biol. Chem.* 256:3951–3955.

Dehlinger, P. J., P. C. Jost, and O. H. Griffith. 1974. Lipid binding to the amphipathic membrane protein cytochrome b_5. *Proc. Natl. Acad. Sci. USA.* 71:2280–2284.

De Kruijff, B., and E. J. J. Van Zoelen. 1978. Effect of the phase transition on the transbilayer movement of dimyristoyl phosphatidylcholine in unilamellar vesicles. *Biochim. Biophys. Acta.* 511:105–115.

Enoch, H. G., P. J. Fleming, and P. Strittmatter. 1979. The binding of cytochrome b_5 to phospholipid vesicles and biological membranes. Effect of orientation on intermembrane transfer and digestion by carboxypeptidase Y. *J. Biol. Chem.* 254:6483–6488.

Enoch, H. G., and P. Strittmatter. 1979. Formation and properties of 1000 Å-diameter, single-bilayer phospholipid vesicles. *Proc. Natl. Acad. Sci. USA.* 76:145–149.

Everett, J., A. Zlotnick, J. Tennyson, and P. W. Holloway. 1986. Fluorescence quenching of cytochrome b_5 in vesicles with an asymmetric transbilayer distribution of brominated phosphatidylcholine. *J. Biol. Chem.* 261:6725–6729.

Fleming, P. J., D. E. Koppel, A. L. Y. Lau, and P. Strittmatter. 1979. Intramembrane position of the fluorescent tryptophanyl residue in membrane-bound cytochrome b_5. *Biochemistry.* 18:5458–5464.

Franks, N. P., and W. R. Lieb. 1979. The structure of lipid bilayers and the effects of general anaesthetics. An x-ray and neutron diffraction study. *J. Mol. Biol.* 133:469–500.

Franks, N. P., and Y. K. Levine. 1981. Low angle x-ray diffraction. *In* Membrane Spectroscopy. E. Grell, editor. Springer-Verlag, New York. 437–487.

Freire, E., T. Markello, C. Rigell, and P. Holloway. 1983. Calorimetric and fluorescence characterization of interactions between cytochrome b_5 and phosphatidylcholine bilayers. *Biochemistry.* 22:1675–1680.

George, R., R. N. A. H. Lewis, and R. N. McElhaney. 1990. Studies on the purified Na^+, Mg^{2+}-ATPase from acholeplasma laidlawii B

membranes: a differential scanning calorimetric study of the protein-phospholipid interactions. *Biochem. Cell Biol.* 68:161–168.

Gogol, E. P., and D. M. Engelman. 1984. Neutron scattering shows that cytochrome b_5 penetrates deeply into the lipid bilayer. *Biophys. J.* 46:491–495.

Gogol, E. P., D M. Engelman, and G. Zaccai. 1983. Neutron diffraction analysis of cytochrome b_5 reconstituted in deuterated lipid multilayers. *Biophys. J.* 43:285–292.

Gomez-Fernandez, J. C., F. M. Goni, D. Bach, C. J. Restall, and D. Chapman. 1980. Protein-lipid interaction. Biophysical studies of $(Ca^{2+} + Mg^{2+})$-ATPase in reconstituted systems. *Biochim. Biophys. Acta.* 598:502–516.

Herbette, L. G., P. DeFoor, S. Fleischer, D. Pascolini, A. Scarpa, and J. K. Blasie. 1985. The separate profile structure of the functional calcium pump protein and the phospholipid bilayer within isolated sarcoplasmic reticulum membranes determined by x-ray and neutron diffraction. *Biochim. Biophys. Acta.* 817:103–122.

Herbette, L. G., J. Marquardt, A. Scarpa, and J. K. Blasie. 1977. A direct analysis of lamellar x-ray diffraction from hydrated oriented multilayers of fully functional sarcoplasmic reticulum. *Biophys. J.* 20:245–272.

Holloway, P. W., and C. Bucheit. 1990. The structure of the hydrophobic domain of cytochrome b_5 by infrared spectroscopy. *Biophys. J.* 57:464*a*. (Abstr.)

Holloway, P. W., and H. H. Mantsch. 1989. Structure of cytochrome b_5 in solution by Fourier-transform infrared spectroscopy. *Biochemistry.* 28:931–935.

Jeffcoat, R., and A. T. James. 1984. The regulation of desaturation and elongation of fatty acids in mammals. *In* Fatty Acid Metabolism and Its Regulation. S. Numa, editor. *New Compr. Biochem.* 7:85–112.

Keyes, S. R., J. A. Alfano, I. Jansson, and D. L. Cinti. 1979. Rat liver microsomal elongation of fatty acids. Possible involvement of cytochrome b_5. *J. Biol. Chem.* 254:7778–7784.

Ladohkin, A. S., L. Wang, A. W. Steggles, and P. W. Holloway. 1991. Fluorescence study of a mutant cytochrome b_5 with a single tryptophan in the membrane binding domain. *Biophys. J.* 59:359*a*. (Abstr.)

Lee, T. C., R. C. Baker, N. Stephens, and F. Snyder. 1977. Evidence for participation of cytochrome b_5 in microsomal delta-desaturation of fatty acids. *Biochim. Biophys. Acta.* 489:25–31.

Luzzati, V., A. Tardieu, and D. Taupin. 1972. A pattern recognition approach to the phase problem: application to the x-ray diffraction study of biological membranes and model systems. *J. Mol. Biol.* 64:269–286.

Markello, T., A. Złotnick, J. Everett, J. Tennyson, and P. W. Holloway. 1985. Determination of the topography of cytochrome b_5 in lipid vesicles by fluorescence quenching. *Biochemistry.* 24:2895–2901.

Mathews, F. S., E. W. Czerwinski, and P. Argos. 1979. The x-ray crystallographic structure of calf liver cytochrome b_5. *In* The Porphyrins. Vol. VII. D. Dolphin, editor. Academic Press, Inc., New York. 107–146.

McElhaney, R. N. 1982. The use of differential scanning calorimetry and differential thermal analysis in studies of model and biological membranes. *Chem. Phys. Lipids.* 30:229–259.

McElhaney, R. N. 1986. Differential scanning calorimetric studies of lipid-protein interactions in model membrane systems. *Biochim. Biophys. Acta.* 864:361–421.

McIntosh, T. J., and S. A. Simon. 1986. Hydration force and bilayer deformation: a reevaluation. *Biochemistry.* 25:4058–4066.

Mollay, C. 1976. Effect of melittin and melittin fragments on the thermotropic phase transition of dipalmitoyllecithin and on the amount of lipid-bound water. FEBS (*Fed. Eur. Biochem. Soc.*) *Lett.* 64:65–68.

Moody, M. F. 1963. X-ray diffraction pattern of nerve myelin: a method for determining the phases. *Science* (Wash. DC). 142:1173–1174.

Okayasu, T., T. Ono, K. Shinojima, and Y. Imai. 1977. Involvement of cytochrome b_5 in oxidative desaturation of linoleic acid to γ-linolenic acid in rat liver microsomes. *Lipids.* 12:267–271.

Oldfield, E., R. Gilmore, M. Glaser, H. S. Gutowsky, J. C. Hshung, S. Y. Kang, T. E. King, M. Meadows, and D. Rice. 1978. Deuterium nuclear magnetic resonance investigation of the effects of proteins and polypeptides on hydrocarbon chain order in model membrane systems. *Proc. Natl. Acad. Sci. USA.* 75:4657–4660.

Ozols, J. 1989. Structure of cytochrome b_5 and its topology in the microsomal membrane. *Biochim. Biophys. Acta.* 997:121–130.

Pachence, J. M., R. Fischetti, and J. K. Blasie. 1989. Location of the Heme-Fe atoms within the profile structure of a monolayer of cytochrome *c* bound to the surface of an ultrathin lipid multilayer film. *Biophys. J.* 56:327–337.

Pachence, J. M., S. Amador, G. Maniara, J. Vanderkooi, P. L. Dutton, and J. K. Blasie. 1990. Orientation and lateral mobility of cytochrome *c* on the surface of ultrathin lipid multilayer films. *Biophys. J.* 58:379–389.

Papahadjopoulos, D., M. Moscarello, E. H. Eylar, and T. Isac. 1975. Effects of proteins on thermotropic phase transitions of phospholipid membranes. *Biochim. Biophys. Acta.* 401:317–335.

Pearson, R. H., I. Pascher. 1979. The molecular structure of lecithin dihydrate. *Nature* (*Lond.*) 281:499–501.

Reddy, V. R., P. Kupfer, and E. Caspi. 1977. Mechanism of C-5 double bond introduction in the biosynthesis of cholesterol by rat liver microsomes. *J. Biol. Chem.* 252:2797–2801.

Rzepecki, L. M., P. Strittmatter, and L. G. Herbette. 1986. X-ray diffraction analysis of cytochrome b_5 reconstituted in egg phosphatidylcholine vesicles. *Biophys. J.* 49:829–838.

Skita, V., M. Filipkowski, A. F. Garito, and J. K. Blasie. 1986*a*. Profile structures of very thin multilayers by x-ray diffraction using direct and refinement methods of analysis. *Phys. Review B.* 34:5826–5837.

Skita, V., W. Richardson, M. Filipkowski, A. Garito, and J. K. Blasie. 1986*b*. Overlayer-induced ordering of the disordered surface monolayer in langmuir-blodgett multilayer thin films. *J. Physique.* 47:1849–1855.

Spatz, L., and P. Strittmatter. 1971. A form of cytochrome b_5 that contains an additional hydrophobic sequence of 40 amino acid residues. *Proc. Natl. Acad. Sci. USA.* 68:1042–1046.

Strittmatter, P., and H. A. Dailey. 1982. Essential structural features and orientation of cytochrome b_5 in membranes. *In* Membranes and Transport. Vol. 1. A. N. Martonosi, editor. Plenum Publishing Co., New York. 71–82.

Strittmatter, P., and M. J. Rogers. 1975. Apparent dependence of interactions between cytochrome b_5 and cytochrome b_5 reductase upon translational diffusion in dimyristoyl lecithin liposomes. *Proc. Natl. Acad. Sci. USA.* 72:2658–2661.

Strittmatter, P., L. Spatz, D. Corcoran, M. J. Rogers, B. Setlow, and R. Redline. 1974. Purification and properties of rat liver microsomal stearyl coenzyme A desaturase. *Proc. Natl. Acad. Sci. USA.* 71:4565–4569.

Takagaki, Y., R. Radhakrishnan, C. M. Gupta, and H. G. Khorana. 1983*a*. The membrane-embedded segment of cytochrome b_5 as studied by cross-linking with photoactivatable phospholipids. I. The transferable form. *J. Biol. Chem.* 258:9128–9135.

Takagaki, Y., R. Radhakrishnan, K. W. A. Wirtz, and H. G. Khorana. 1983*b*. The membrane-embedded segment of cytochrome b_5 as studied by cross-linking with photoactivatable phospholipids. II. The nontransferable form. *J. Biol. Chem.* 258:9136–9142.

Tennyson, J., and P. W. Holloway. 1986. Fluorescence studies of cytochrome b_5 topography. Incorporation of cytochrome b_5 into brominated phosphatidylcholine vesicles by deoxycholate. *J. Biol. Chem.* 261:14196–14200.

Ungar, G., and J. L. Feijoo. 1990. Simultaneous x-ray diffraction and differential scanning calorimetry (XDDSC) in studies of molecular and liquid crystals. *Mol. Cryst. Liq. Cryst.* 180B:281–291.

Veitch, N. C., D. W. Concar, R. J. P. Williams, and D. Whitford. 1988. Investigation of the solution structures and mobility of oxidized and reduced cytochrome b_5 by 2D NMR spectroscopy. FEBS (*Fed. Eur. Biochem. Soc.*) Lett. 238:49–55.

Verma, S. P., D. F. H. Wallach, and I. C. P. Smith. 1974. The action of melittin on phosphatide multibilayers as studied by infrared dichroism and spin labeling. A model approach to lipid-protein interactions. *Biochim. Biophys. Acta.* 345:129–140.

Wiener, M. C., and S. H. White. 1991*a*. Fluid bilayer structure determination by the combined use of x-ray and neutron diffraction. I. Fluid bilayer models and the limits of resolution. *Biophys. J.* 59:162–173.

Wiener, M. C., and S. H. White. 1991*b*. Transbilayer distribution of bromine in fluid bilayers containing a specifically brominated analogue of dioleoylphosphtidylcholine. *Biochemistry.* 30:6997–7008.

Williams, I. C., and R. M. Bell. 1972. Membrane matrix disruption by melittin. *Biochim. Biophys. Acta.* 288:255–262.

Worthington, C. R. 1969. The interpretation of low-angle x-ray data from planar and concentric multilayered structures. The use of one-dimensional electron density strip models. *Biophys. J.* 9:222–234.

Worthington, C. R., and R. S. Khare. 1978. The structure determination of lipid bilayers. *Biophys. J.* 23:407–425.

Young, H. S., V. Skita, R. P. Mason, and L. G. Herbette. 1991. Molecular basis for the noncompetitive inhibition of 1,4-dihydropyridine calcium channel drug binding in cardiac sarcolemmal membranes. *Biophys. J.* 61:1244–1255.